

Design of Pv System With Multilevel Structures for Generation of Higher Number of Voltage Levels

Durga Prasad.V & A.Srikanth

¹M.Tech (student), ST. Martin's Engineering College Affiliated to JNTUH, Hyderabad, Telangana, India.
Area of interest includes Power Electronics.

²Assistant Professor, ST. Martin's Engineering College Affiliated to JNTUH, Hyderabad, Telangana, India. Area of interest includes Power Electronics.

Abstract—A new method of generating higher number of voltage levels by stacking multilevel converters of lower space vector structures and having a single DC power supply as mentioned above with low voltage devices is presented in this paper. A photovoltaic system, also PV system or solar power system, is a power system designed to supply usable solar power by means of photovoltaics. An important feature of this stacked structure is the use of low voltage devices while attaining higher number of levels. This will find extensive applications in electric vehicles since direct battery drive is possible. Stacked multi-cell converter was introduced to generate more levels. They use less number of capacitors but require more switches. Solar PV has specific advantages as an energy source: its operation generates no pollution and no greenhouse gas emissions once installed. The voltages of all the capacitors in the structure can be controlled within a switching cycle using the switching state redundancies (pole voltage redundancies). This helps in reducing the capacitor size. Also, the capacitor voltages can be balanced irrespective of modulation index and load power factor. A 9-level inverter is developed by stacking two 5-level inverters and an induction motor is run using V/f control scheme. By using the simulation results we can analyze the proposed method at both the steady state and transient state.

Index Terms—Active power control, constant power control, maximum power point tracking, PV systems, power converters.

INTRODUCTION

Photovoltaic (PV) power generation is becoming more promising since the introduction of the thin film PV technology due to its lower cost, excellent high temperature performance, low weight, flexibility, and glass-free easy installation. The multilevel inverter is more popular than a conventional two-level inverter, because the medium voltage rating power semiconductor devices may be employed for high power application along with higher power quality. In order to obtain better waveform quality and lower total harmonic distortion (THD) in the phase voltages, they also have advantages of reduced Electro-magnetic interference (EMI), lower device voltage ratings and lower switching frequency. Hence they found widespread applications in motor drives, grid tied converters, high voltage DC transmission, reactive power compensation, wind energy

conversion and in many other high power applications [2]. Basic multilevel topologies include diode clamped multilevel inverter (DC-MLI), flying capacitor inverter (FC) and cascaded H-bridge inverter (CHB)[2],[3]. Three level DCMLI, commonly known as neutral point clamped inverters (NPC) have become popular in industry. But for higher levels more clamping diodes are needed and also balancing the capacitors for entire modulation range is an issue [3]. To overcome the loss balancing problem, a modified version of NPC, known as the active NPC (ANPC) is introduced wherein the clamping diodes are replaced with the switches for balancing losses among the switches [5]. FCs are another class of MLCs where in several charged capacitors are used in generating higher number of voltage levels.

A photovoltaic system, also PV system or solar power system, is a power system designed to supply usable solar power by means of photovoltaics. It consists of an arrangement of several components, including solar panels to absorb and convert sunlight into electricity, a solar inverter to change the electric current from DC to AC, and mounting cabling and other electrical accessories to set up a working system.

The main focus of the paper is, to improve the power quality and reduce the power switch count along with maximum blocking voltage in symmetric configuration is discussed. The input dc source can be provided through a multi-winding transformer or photovoltaic panel with dc/dc converter. This paper focused on the new hybrid multilevel inverter with novel carrier based modulation technique to minimize the output voltage harmonic profile. In order to obtain a better quality output voltage or current waveform, the switching frequency needs to increase in the conventional 2-level and 3-level inverters. But in high voltage and high power applications, there is a limitation on switching frequency due to the associated switching losses and power dissipation. Increasing the number of levels in the output voltage, reduces harmonic distortion in the

output phase voltage waveform[1]. Multilevel converters (MLC) are capable of generating higher levels in the output voltage waveform with low voltage stress on the switches.

This paper proposes a new method of generating higher number of levels in the voltage waveform by stacking multilevel converters with lower voltage space vector structures. Another breed of power converters are the CHB converters[2]. They have the least component count compared to DCMLIs and FCs especially due to absence of any clamping diodes or flying capacitors. But CHB based topologies reported with single DC supply and multiple floating capacitors in each phase are dependent on load power factor and modulation index for the floating capacitor balancing.

INVERTER TOPOLOGY AND ITS OPERATION

Each of the 5-level inverters are obtained by cascading a 3-level flying capacitor inverter and a capacitor fed H-bridge. There are 2 selector switches in each phase to connect the respective outputs to the induction machine.

The proposed inverter structure for a 9-level is shown in Fig. 1(a). It is realized by stacking two 5-level inverters in each phase.

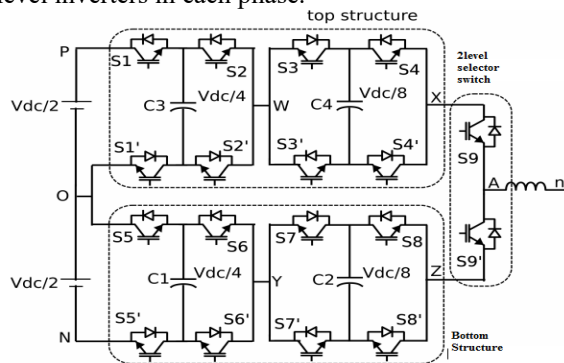


Figure 1. Power circuit for the proposed stacked 9-level inverter and its modulating signal for phase 'a'.
(a) Proposed 9 level inverter by stacking two 5 level inverters

The flying capacitor in each structure has to be maintained at $V_{dc}/4$ and H bridge capacitors have to be maintained at $V_{dc}/8$, where V_{dc} is the DC link for a conventional 2-level inverter. The structure overall has 9 pairs of complimentary switches in each phase ($S1-S1'$, $S2-S2'$... $S9-S9'$). Each of the switches in FC needs to block only $V_{dc}/4$ and each of the switches in H-bridge needs to block only $V_{dc}/8$.

During the positive half cycle of the reference waveform (signal-1 in Fig. 1(b)), the bottom structure is clamped to the mid point 'O' by turning on $S5, S6, S7, S8$. Because of this operation,

the voltage rating of $S9'$ has to be $V_{dc}/2$ only. The selector switches $S9$ is kept on and $S9'$ is off during this period. Now the top structure will switch to generate the required pole voltages. Similarly during the negative half cycle (signal-2 in Fig. 1(b)), the top inverter structure is clamped to the mid point 'O' by turning on $S1', S2', S3', S4'$. $S9$ is kept on and $S9'$ is permanently kept off. Again $S9$ has to be rated for only $V_{dc}/2$.

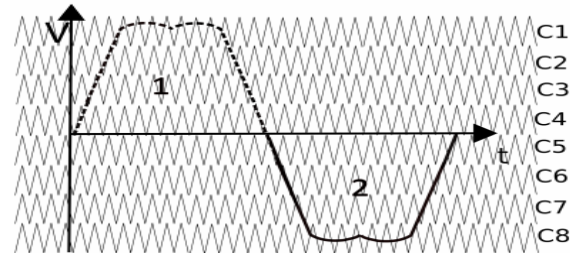


Figure 1. Power circuit for the proposed stacked 9-level inverter and its modulating signal for phase 'a'.
(b) Signal 1 for modulating the top structure and signal 2 for modulating the bottom structure along with the 8 carriers

Here the bottom structure will switch to generate the required pole voltages. So the selector switches are switching at line frequency only. The selector switches switch only during the zero crossing of the modulating signal. When the modulating signal is transiting from positive half cycle to negative half cycle, the upper selector switch has to go off and bottom selector switch has to turn on. During this transition, it can be seen that all the top switches of the bottom structure ($S5, S6, S7, S8$) and all the bottom switches of the top structure ($S1', S2', S3', S4'$) are on. If $S9'$ is turned on just before $S9$ turns off, $S9$ can undergo a zero voltage switching off. At the same time, $S9'$ is undergoing a zero voltage switching on as shown in Fig. 2. The darkened switches in the figure are on.

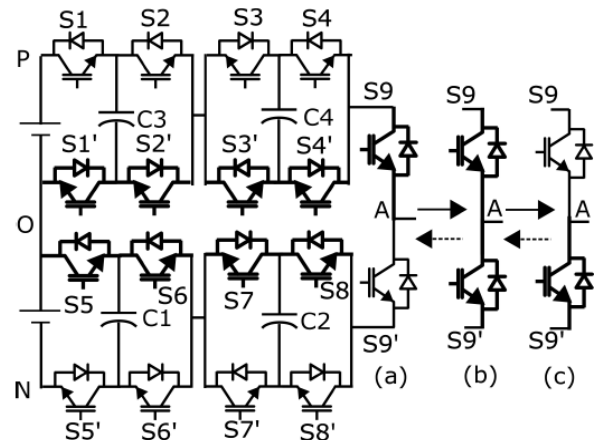


Figure 2. Transition states during zero crossing of

modulating signal to eliminate switching loss in the selector switches.

The solid arrow shows transition from positive to negative half cycle. The dotted arrow shows transition from negative to positive half cycle. All the darkened switches are on. Also this inverter has a modular structure, since the H bridges can be bypassed if it fails and the inverter can still operate in the entire modulation range with lower number of voltage levels.

CAPACITOR VOLTAGE BALANCING

The capacitor voltages need to be maintained at the respective levels for generating the pole voltages. Each of the capacitor voltages in the topology has to be maintained at their reference values. Hence we define a small hysteresis band for each of the capacitor voltage references and maintains the voltages within this band using the available switching state redundancies. During a sampling instant, if the capacitor charges and reaches the upper limit of the hysteresis band, immediately in the next sampling instant, the switching state is changed to discharge that capacitor. Since the capacitors are designed considering the switching frequency, peak of load current and the voltage deviation, the capacitor voltages always lie within the hysteresis band.

Table I list all the switching redundancies of all the pole voltages and also their effect on the capacitor voltages for a particular direction of current.

Table I
SWITCHING STATE REDUNDANCIES FOR THE POLE VOLTAGES AND THEIR EFFECT ON THE CAPACITOR VOLTAGES.

| S.No | Switch States | V_{AN} | I_a | C1 | C2 |
|------|---------------|-------------|-------|----|----|
| 1 | 0000 0000 0 | 0 | + | U | U |
| 2 | 0000 0011 0 | 0 | + | U | U |
| 3 | 0000 0001 0 | $V_{dc}/8$ | + | U | D |
| 4 | 0000 0110 0 | $V_{dc}/8$ | + | D | C |
| 5 | 0000 1010 0 | $V_{dc}/8$ | + | C | C |
| 6 | 0000 0100 0 | $V_{dc}/4$ | + | D | U |
| 7 | 0000 0111 0 | $V_{dc}/4$ | + | D | U |
| 8 | 0000 1000 0 | $V_{dc}/4$ | + | C | U |
| 9 | 0000 1011 0 | $V_{dc}/4$ | + | C | U |
| 10 | 0000 0101 0 | $3V_{dc}/8$ | + | D | D |
| 11 | 0000 1001 0 | $3V_{dc}/8$ | + | C | D |
| 12 | 0000 1110 0 | $3V_{dc}/8$ | + | U | C |
| 13 | 0000 1100 0 | $V_{dc}/2$ | + | U | U |
| 14 | 0000 1111 0 | $V_{dc}/2$ | + | U | U |
| 15 | 0000 1111 1 | $V_{dc}/2$ | + | U | U |
| 16 | 0011 1111 1 | $V_{dc}/2$ | + | U | U |
| 17 | 0001 1111 1 | $5V_{dc}/8$ | + | U | D |
| 18 | 0110 1111 1 | $5V_{dc}/8$ | + | D | C |
| 19 | 1010 1111 1 | $5V_{dc}/8$ | + | C | C |
| 20 | 0100 1111 1 | $3V_{dc}/4$ | + | D | U |
| 21 | 0111 1111 1 | $3V_{dc}/4$ | + | D | U |
| 22 | 1000 1111 1 | $3V_{dc}/4$ | + | C | U |
| 23 | 1011 1111 1 | $3V_{dc}/4$ | + | C | U |
| 24 | 0101 1111 1 | $7V_{dc}/8$ | + | D | D |
| 25 | 1001 1111 1 | $7V_{dc}/8$ | + | C | D |
| 26 | 1110 1111 1 | $7V_{dc}/8$ | + | U | C |
| 27 | 1100 1111 1 | V_{dc} | + | U | U |
| 28 | 1111 1111 1 | V_{dc} | + | U | U |

As the current reverses, the effect on capacitor voltages also reverses. Fig. 3 shows the use of switching state redundancies to charge and discharge a capacitor for a pole voltage (V_{AN}) of $5V_{dc}/8$. For obtaining $5V_{dc}/8$, the top structure only needs to operate. Hence only top structure is shown in Fig. 3. From the Table I, it can be seen that for the positive direction of current from 'A' to 'n', the switching state (0001 1111 1) discharges C4 while C3 is unaffected which is shown in Fig. 3(a). To charge C4, the switching state (0110 1111 1) is used but it discharges C3 which is shown in Fig. 3(b). Again to charge C3, the switching state (1010 1111 1) is used but it charges C4 also which is shown in Fig. 3(c).

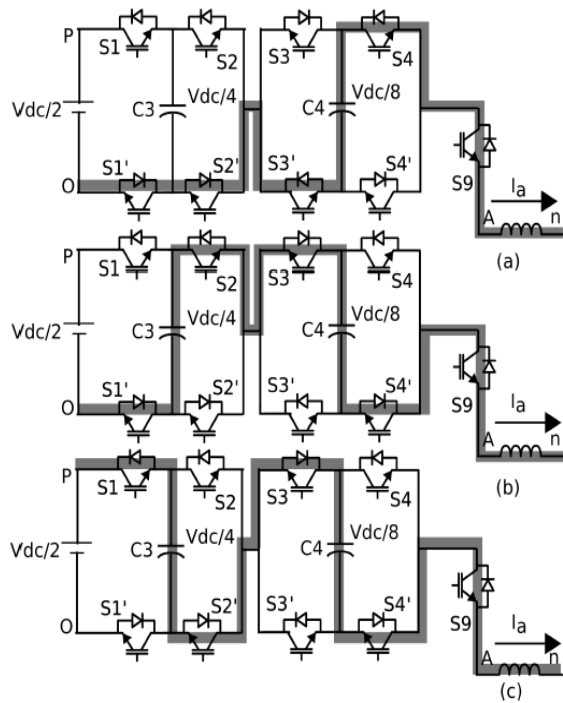


Figure 3. Switching redundancies available for a pole voltage. (a), (b) and (c) show current paths and charge and discharge of capacitors for switching redundancies available for pole voltage of $5V_{dc}/8$

Whenever the capacitor voltages crosses the hysteresis limits, switching states need to change to maintain the capacitor voltages to desired values. For pole voltages of 0, $V_{dc}/2$ and V_{dc} , none of the capacitors are affected due to the current flow. For all other pole voltages, capacitor voltages change with current flow

Again the application of switching state depends on the present state of capacitor voltages and the current directions. Hence all the 12 capacitor voltages and currents are sensed. All the capacitor voltages are compared with their references and capacitor voltage status whether it has exceeded the upper or lower limit of the hysteresis band is given by H_{ax} , where $x = 1,2,3,4$ respectively for C1, C2, C3 and C4. $H_{ax} = '1'$ implies capacitor needs discharging and $H_{ax} = '0'$ implies capacitor needs charging to maintain the capacitor voltages within the hysteresis band. Capacitor voltage status, the required pole voltage and the current direction decide the switching state at any instant.

Table II tells which switching state needs to be applied at any instant depending on the above factors. Thus instantaneous capacitor voltage control using switch state redundancies are possible within inverter switching cycle. This is also independent of load power factor.

Table II

SWITCHING STATE SELECTION TABLE BASED ON CURRENT DIRECTION AND CAPACITOR VOLTAGE STATUS FOR PHASE 'A'

| I_a | H_{a1}/H_{a3} | H_{a2}/H_{a4} | Switching state selection for the various pole voltages | | | | | |
|-------|-----------------|-----------------|---|-------------|-------------|-------------|-------------|-------------|
| | | | $V_{dc}/8$ | $V_{dc}/4$ | $3V_{dc}/8$ | $5V_{dc}/8$ | $3V_{dc}/4$ | $7V_{dc}/8$ |
| + | 0 | 0 | 0000 1010 0 | 0000 1011 0 | 0000 1110 0 | 1010 1111 1 | 1011 1111 1 | 1110 1111 1 |
| + | 0 | 1 | 0000 0001 0 | 0000 1011 0 | 0000 1001 0 | 0001 1111 1 | 1011 1111 1 | 1001 1111 1 |
| + | 1 | 0 | 0000 0110 0 | 0000 0111 0 | 0000 1110 0 | 0110 1111 1 | 0111 1111 1 | 1110 1111 1 |
| + | 1 | 1 | 0000 0001 0 | 0000 0111 0 | 0000 0101 0 | 0001 1111 1 | 0111 1111 1 | 0101 1111 1 |
| - | 0 | 0 | 0000 0001 0 | 0000 0111 0 | 0000 0101 0 | 0001 1111 1 | 0111 1111 1 | 0101 1111 1 |
| - | 0 | 1 | 0000 0110 0 | 0000 0111 0 | 0000 1110 0 | 0110 1111 1 | 0111 1111 1 | 1110 1111 1 |
| - | 1 | 0 | 0000 0001 0 | 0000 1011 0 | 0000 1001 0 | 0001 1111 1 | 1011 1111 1 | 1001 1111 1 |
| - | 1 | 1 | 0000 1010 0 | 0000 1011 0 | 0000 1110 0 | 1010 1111 1 | 1011 1111 1 | 1110 1111 1 |

GENERALIZATION

In the proposed 9-level inverter shown in Fig. 1(a), two 5-level inverters are stacked and each 5-level inverter is generating half of the total inverter pole voltage. During the positive half cycle of the reference modulating signal (trace-2 of of Fig. 11), the top selector switch is on and during the negative half cycle, the bottom selector switch is on, to connect the respective 5-level stacked inverter modules to the output. The gate signal to the top

selector switch is shown in trace-3 of Fig 11. To reduce the number of switches, the structure in Fig. 1(a) can be modified as shown in

COMPARISON WITH OTHER INVERTER TOPOLOGIES

The modified 9-level inverter in Fig. 4 is compared with other existing 9-level topologies in this section.

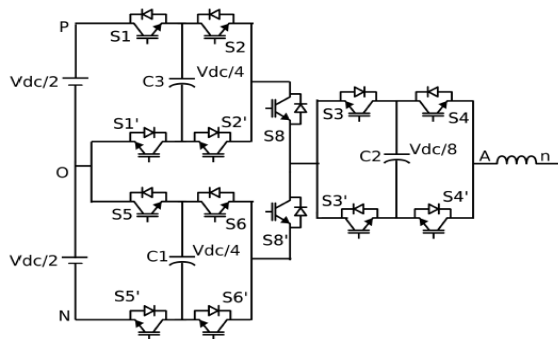


Figure 4. Modified power circuit to reduce number of switches for the proposed stacked 9-level inverter topology for phase ‘a’.

Fig. 4. Here the H bridge is made common to both the FC and selector switch is connected in between. Here the H-bridge switches need to switch throughout the cycle. But they need to block voltage of $V_{dc}/8$ only (same as that in Fig. 1(a)). Therefore the switching losses are controlled. Also by using redundant H-bridges, the system reliability can be improved. This method of stacking can be extended to obtain higher voltage levels.

The modified proposed topology requires total of 42 switches. Out of which, six selector switches are switching at line frequency and whose switching losses can be minimized using the method discussed in the earlier section. The top and bottom FC is operating only for one half of a fundamental cycle and is idle during the other half. In the conventional NPC and FC topologies for 9-level, many clamping diodes and flying capacitors are required for their operation respectively. In the proposed structure with less number of floating capacitors, capacitor balancing can be done throughout the modulation range irrespective of any load power factor, whereas in a 9-level NPC, there is a limitation on modulation index due to the capacitor unbalance problem.

In Fig. 5, a 49-level inverter is shown which is developed by stacking 3 FC and cascading with 3 capacitor fed H-bridges (which are of lower voltage ratings) through a 3-level selector switch. It is shown that a FC cascaded with 3 H-bridges can generate 17 levels. Since there are 3 stacked 17-level inverters, the reference signal has to be divided into three parts

and each will be used for modulating each of the 17-level inverter formed by cascading 3 capacitor fed H-bridges with a FC. Also due to the higher number of voltage levels, switching frequency can be reduced and therefore higher efficiency is achievable. These advantages will make the stacked inverter structure suitable for application in electric vehicles where the inverter can be driven directly from the stacked low voltage batteries.

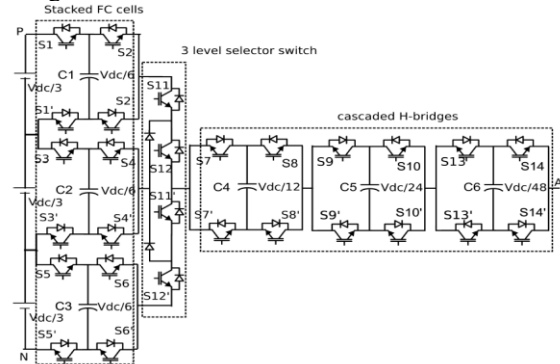


Figure 5. Power circuit schematic for generation of 49 levels by stacking three FC and cascading with three capacitor fed H-bridges of low voltage ratings

The basic conventional CHB structure, although requires least number of components among the conventional topologies, needs more number of isolated dc sources. The open end 9-level configuration uses lesser number of switches but it has twelve $V_{dc}/2$ switches which have to operate throughout the cycle whereas in the proposed inverter, there are only six $V_{dc}/2$ switches (selector switches) and they switch only once in a fundamental cycle and their switching losses are also minimized. In addition, all the $V_{dc}/4$ switches in the FC of the proposed inverter operate only in one half of fundamental cycle unlike in the case of an open end configuration. Again comparing with the standard 9-level ANPC, the switching losses in the $V_{dc}/2$ switches (selector switches) in the proposed inverter (6 compared to 12 in ANPC) are highly minimized with zero voltage switching. Also the $V_{dc}/4$ switches in the proposed inverter (although 24 in number) operate only in one half of fundamental cycle. The comparison is detailed in Table III.

Table III
COMPARISON OF 9-LEVEL INVERTER TOPOLOGIES

| Topologies | IGBT | | | capacitors | | | | Clamping diodes | DC sources | | |
|------------------|-------|-------|-------|------------|-------|---------|-------|-----------------|------------|-------|-------|
| | Vdc/2 | Vdc/4 | Vdc/8 | Vdc/4 | Vdc/8 | 3 Vdc/8 | Vdc/2 | | vdc | Vdc/2 | Vdc/8 |
| proposed | 6 | 24 | 12 | 6 | 3 | 0 | 0 | 0 | 0 | 2 | 0 |
| NPC | 0 | 0 | 48 | 0 | 8 | 0 | 0 | 168 | 1 | 0 | 0 |
| FC | 0 | 0 | 48 | 0 | 84 | 0 | 0 | 0 | 1 | 0 | 0 |
| Conventional CHB | 0 | 0 | 48 | 0 | 0 | 0 | 0 | 0 | 0 | 0 | 12 |
| Open end 9L | 12 | 12 | 12 | 0 | 9 | 0 | 0 | 0 | 0 | 2 | 0 |
| Standard 9L-ANPC | 12 | 0 | 24 | 3 | 3 | 3 | 0 | 0 | 0 | 2 | 0 |

PV SOURCE

Photovoltaics (PV) covers the conversion of light into electricity using semiconducting materials that exhibit the photovoltaic effect, a phenomenon studied in physics, photochemistry, and electrochemistry. The dynamic model of PV cell is shown in below Fig.6.

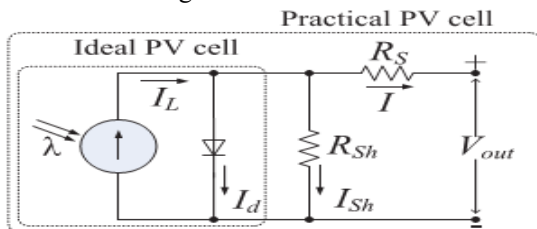


Fig 6. Equivalent electrical circuit of the PV cell. The basic equation describing the I -V characteristic of a practical PV cell is

$$I = I_L - I_d - I_{sh} = I_L - I_D \left[e^{\frac{QV_{oc}}{AKT}} - 1 \right] - \frac{V_{out} + IR_s}{R_{sh}} \quad (1)$$

where \$I_D\$ is the saturation current of the diode, \$Q\$ is the electron charge, \$A\$ is the curve fitting constant (or diode emission factor), \$K\$ is the Boltzmann constant and \$T\$ is the temperature on absolute scale. PV systems convert light directly into electricity and shouldn't be confused with other technologies, such as concentrated solar power or solar thermal, used for heating and cooling.

Photovoltaics (PV) is a term which covers the conversion of light into electricity that exhibit the photovoltaic effect, a phenomenon studied in physics, photochemistry, and electrochemistry. Photovoltaic (PV) power generation is becoming more promising since the introduction of the thin film PV technology due to its lower cost, excellent high temperature performance, low weight, flexibility, and glass-free easy installation.

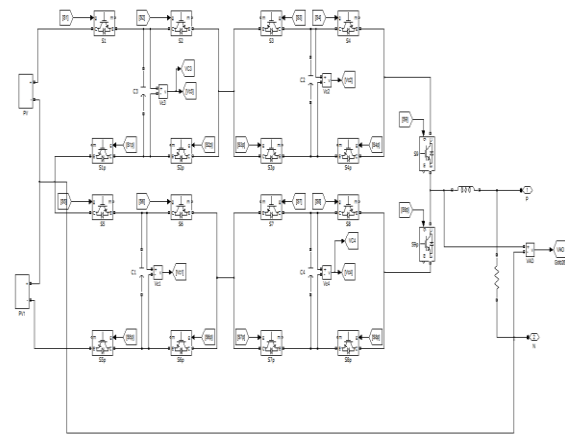


Fig.7. Block diagram of simulation with PV system
The PV system is connected to the proposed inverter structure for a nine-level. It is realized by stacking two five-level inverters in each phase.

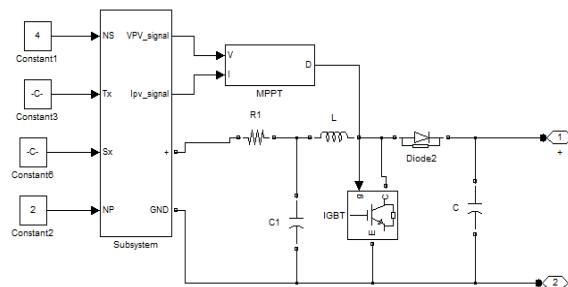
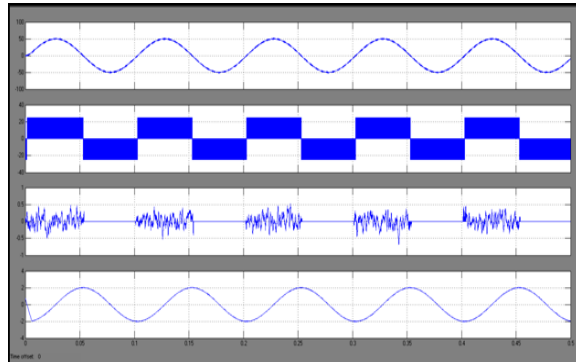


Fig.8. Simulation diagram of PV system
SIMULATION RESULTS

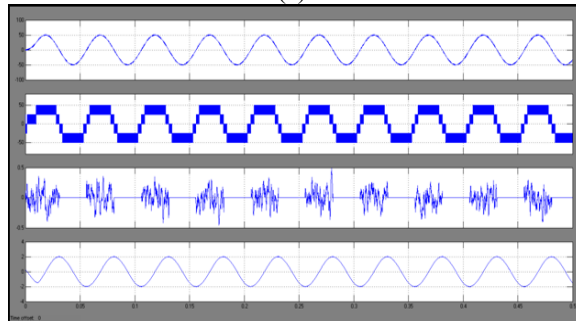
A 3 phase, 415V, 7.5KW, 50 Hz induction motor (IM) is driven with the proposed 9-level inverter shown in Fig. 1(a) using open loop V/f control scheme.

Capacitance value of 2200µF is selected for all the capacitors in the experiment. Synchronous

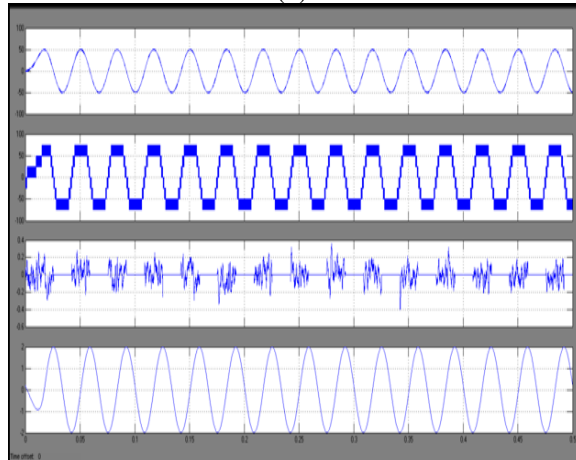
PWM technique is implemented for the proposed inverter.



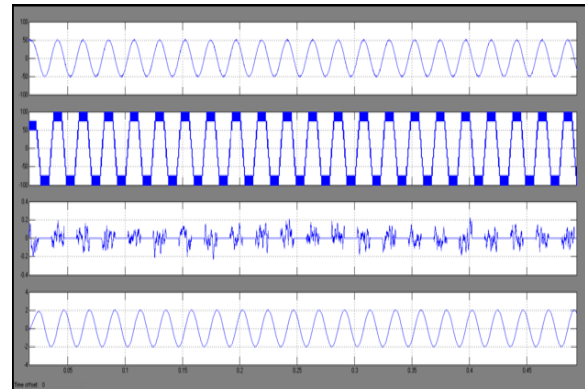
(a)



(b)



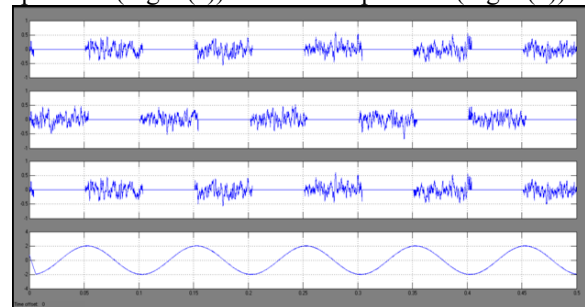
(c)



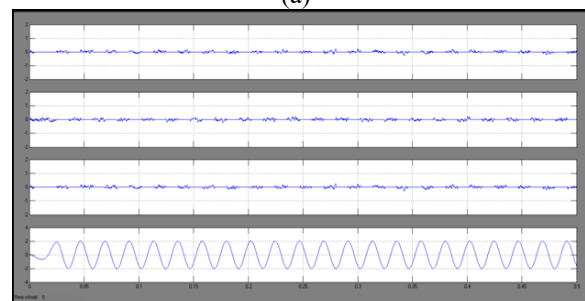
(d)

Figure 9. Motor Phase voltage (V_{AN}), Inverter pole voltage (V_{AO}), Capacitor voltage ripple (V_{c3}), Phase current (I_a) for phase A for different modulation indices. (b), (c) and (d) y-axis 1) V_{AN} : 100V/div, 2) V_{AO} : 100V/div 3) V_{c3} : 5V/div 4) I_a : 2A/div. (a) y-axis 1) V_{AN} : 50V/div, 2) V_{AO} : 50V/div 3) V_{c3} : 5V/div 4) I_a : 2A/div

The results showing the inverter phase voltages (trace-1), pole voltages with respect to midpoint 'O' (trace-2), the flying capacitor voltage ripple of top structure (trace-3) and phase current (trace-4) for 'a' phase are shown for 10 Hz operation (Fig. 7(a)), 20 Hz operation (Fig. 7(b)), 30 Hz operation (Fig. 7(c)) and 45 Hz operation (Fig. 7(d)).



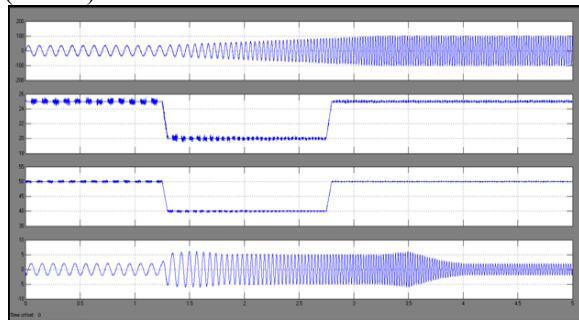
(a)



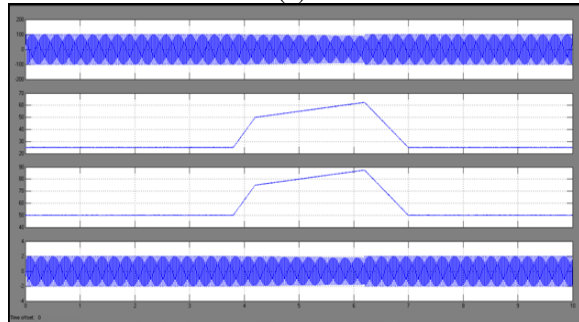
(b)

Figure 10. Capacitor voltages ripple and motor phase current for 'a' phase. y-axis: 1) ΔV_{c1} : 5V/div, 2) ΔV_{c3} : 5V/div, 3) ΔV_{c4} : 5V/div, 4) I_a : 2A/div

It can be seen in the above figures that as the speed command is increased from 10 Hz to 45 Hz, the number of levels in the pole voltage waveform (trace-2) increases from 3 to 9.



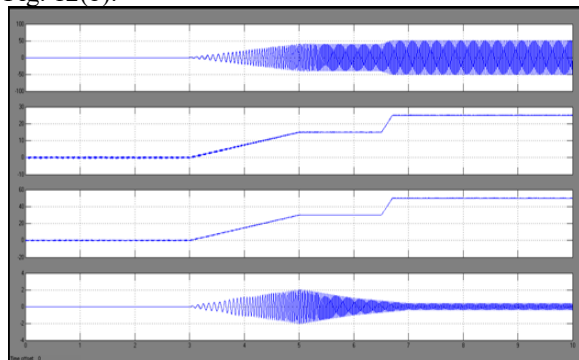
(a)



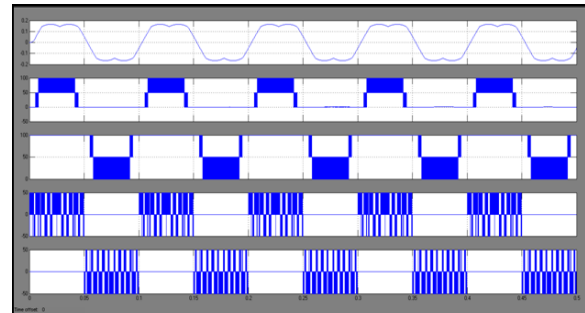
(b)

Figure 11. (a) Motor acceleration. (b) Intentional capacitor unbalancing. yaxes: 1) Motor Phase voltage (VAN), 2) Capacitor voltage Vc4, 3) Capacitor voltage Vc3, 4) Phase current (Ia).

To test the capacitor voltage balancing algorithm, the balancing algorithm is intentionally disabled at Td and then enabled at Te as shown in Fig. 12(b).



(a)



(b)

Figure13. (a) Motor starting transients. y-axis: 1) Motor Phase voltage (VAN), 2) Capacitor voltage Vc3, 3) Capacitor voltage Vc4, 4) Phase current (Ia). (b) Individual FC pole voltages (traces-2,3) and Individual H-bridge switchings (traces-4,5). 1) Modulating signal, 2) VVO, 100V/div, 3) VYO, 100V/div, 4) VXW, 20V/div, 5) VZY, 50V/div.

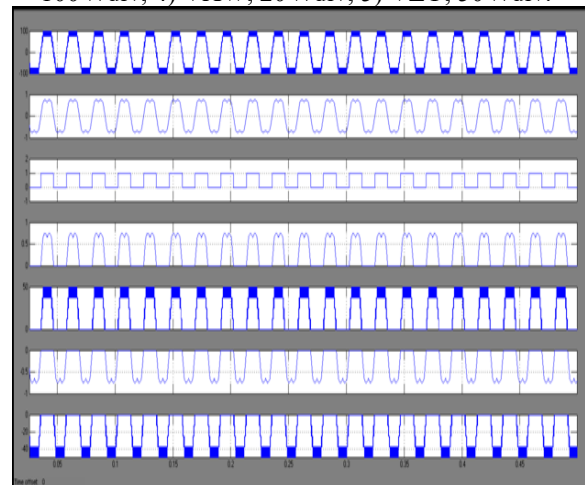


Figure 14. Modulating signals and the generated pole voltages by each of the stacked cells and the inverter at 45 Hz operation. x axis: 10ms/div. 2) VAO, 100V/div, 3) Gating signal, 50V/div, 5) VXO, 100V/div, 7) VZO, 100V/div.

CONCLUSION

This paper proposes a new method of generating higher number of levels in the voltage waveform by stacking multilevel converters with lower voltage space vector structures. Here each of the stacked inverter is having only one DC supply. Solar PV has specific advantages as an energy source: its operation generates no pollution and no greenhouse gas emissions once installed, it shows simple scalability in respect of power needs and silicon has large availability in the Earth's crust. The proposed stacked multilevel inverter has a modular structure which is realized by stacking the FC and cascading it with series connected capacitor fed H-

bridges. The concept of stacking can be generalized to obtain higher voltage levels. As the number of levels increases, blocking voltages of switches reduces and the proposed structure can be fed from low voltage battery cells. Also, higher number of voltage levels imply lower switching frequency and therefore higher efficiency, which makes it suitable for application in electric vehicles. Hysteresis based capacitor voltage balancing algorithm is used to maintain the capacitor voltages irrespective of modulation index and load power factor. By using the simulation results we can analyze the proposed method.

REFERENCES

- [1] A. Nabae, I. Takahashi, and H. Akagi, "A new neutral-point-clamped PWM inverter," *IEEE Trans. Ind. Appl.*, vol. IA-17, no. 5, pp. 518–523, Sept 1981.
- [2] S. Kouro, M. Malinowski, K. Gopakumar, J. Pou, L. Franquelo, B. Wu, J. Rodriguez, M. Perez, and J. Leon, "Recent advances and industrial applications of multilevel converters," *IEEE Trans. Ind. Electron.*, vol. 57, no. 8, pp. 2553–2580, Aug 2010.
- [3] J. Rodriguez, S. Bernet, P. Steimer, and I. Lizama, "A survey on neutralpoint-clamped inverters," *IEEE Trans. Ind. Electron.*, vol. 57, no. 7, pp. 2219–2230, July 2010.
- [4] P. Barbosa, P. Steimer, J. Steinke, L. Meysenc, M. Winkelkemper, and N. Celanovic, "Active neutral-point-clamped multilevel converters," in *Proc. 2005 IEEE Power Electron. Special. Conf.*, June 2005, pp. 2296–2301.
- [5] T. Bruckner, S. Bernet, and H. Guldner, "The active npc converter and its loss-balancing control," *IEEE Trans. Ind. Electron.*, vol. 52, no. 3, pp. 855–868, June 2005.
- [6] H. Wang and F. Blaabjerg, "Reliability of capacitors for dc-link applications in power electronic converters ;an overview," *IEEE Trans. Ind. Appl.*, vol. 50, no. 5, pp. 3569–3578, Sept 2014.
- [7] S. Pulikanti and V. Agelidis, "Hybrid flying-capacitor-based activenneutral- point-clamped five-level converter operated with SHE-PWM," *IEEE Trans. Ind. Electron.*, vol. 58, no. 10, pp. 4643–4653, Oct 2011.
- [8] T. Chaudhuri, P. Steimer, and A. Rufer, "Introducing the common cross connected stage (c3s) for the 5l ANPC multilevel inverter," in *Proc. IEEE Power Electron. Special. Conf.*, June 2008, pp. 167–173
- [9] P. Rajeevan, K. Sivakumar, K. Gopakumar, C. Patel, and H. Abu-Rub, "A nine-level inverter topology for medium-voltage induction motor drive

with open-end stator winding," *IEEE Trans. Ind. Electron.*, vol. 60, no. 9, pp. 3627–3636, Sept 2013.



DURGA PRASAD .V

Completed B.Tech in Electrical & Electronics Engineering in 2014 from S.S Institute of Technology Affiliated to JNTUH, Hyderabad and Pursuing M.Tech form ST. Martin's Engineering College Affiliated to JNTUH, Hyderabad, Telangana, India. Area of interest includes Power Electronics.
E-mail id:durgaprasadd2@gmail.com



A.SRIKANTH

Completed B.Tech in Electrical & Electronics Engineering in 2010 from ST. Martin's Engineering College Affiliated to JNTUH, Hyderabad and M.Tech in Electrical Power Systems in 2013 from ST. Martin's Engineering College Affiliated to JNTUH, Hyderabad. Working as Assistant Professor at ST. Martin's Engineering College, Kompally, Hyderabad, Telangana, India. Area of interest includes **Electrical Power System, power electronic**.
E-mail id: srikanth4888@gmail.com